

# Flexible Informed Trees (FIT\*): Adaptive Batch-Size Approach for Informed Sampling-Based Planner

Liding Zhang<sup>1</sup>, Zhenshan Bing<sup>1</sup>, Kejia Chen<sup>1</sup>, Lingyun Chen<sup>1</sup>, Fan Wu<sup>1</sup>, Peter Krumbholz<sup>2</sup>, Zhilin Yuan<sup>2</sup>, Sami Haddadin<sup>1</sup>, Alois Knoll<sup>1</sup>

**Abstract**—In modern approaches to path planning and robot motion planning, anytime almost-surely asymptotically optimal planners dominate the benchmark of sample-based planners. A notable example is Batch Informed Trees (BIT\*), where planners iteratively determine paths to groups of vertices within the exploration area. However, maintaining a consistent batch size is crucial for initial pathfinding and optimal performance, relying on effective task allocation. This paper introduces Flexible Informed Tree (FIT\*), a novel planner integrating an adaptive batch-size method to enhance task scheduling in various environments. FIT\* employs a flexible approach in adjusting batch sizes dynamically based on the inherent complexity of the planning domain and the current  $n$ -dimensional hyperellipsoid of the system. By constantly optimizing batch sizes, FIT\* achieves improved computational efficiency and scalability while maintaining solution quality. This adaptive batch-size method significantly enhances the planner’s ability to handle diverse and evolving problem domains. FIT\* outperforms existing single-query, sampling-based planners on the tested problems in  $\mathbb{R}^2$  to  $\mathbb{R}^8$ , and was demonstrated in real-world environments with KI-Fabrik/DARKO-Project Europe.

**Index Terms**—adaptive batch-size,  $n$ -dimensional hyperellipsoid, sampling-based planning, informed sampling.

## I. INTRODUCTION

Path planning is vital in robotics, autonomous driving, game design, and related fields. It computes the best route from start to goal while considering obstacles and objectives. Early methods like Dijkstra’s algorithm [1] found the shortest path in a graph. The A\* algorithm [2] combined *graph* and *heuristic* search, enabling faster and more accurate path determination. Anytime Repairing A\* (ARA\*) [3] is an extension of the A\* algorithm for efficient pathfinding. Its *Anytime* feature provides a usable solution progressively during execution, making it suitable for real-time applications. The *Repairing* aspect involves iterative solution enhancement by adjusting search parameters, valuable in dynamic environments for balancing speed and solution quality.

Using graph-based planning in continuous state spaces is challenging due to the need for suitable discretization, known as *prior discretization*. Coarse resolution boosts efficiency but may yield suboptimal paths. Finer resolution improves path quality [4] but demands significantly more computation, especially in high-dimensional environments which known as *the curse of dimensionality* [5]. To tackle this issue, sampling-based planning methods like Rapidly-exploring Random Trees

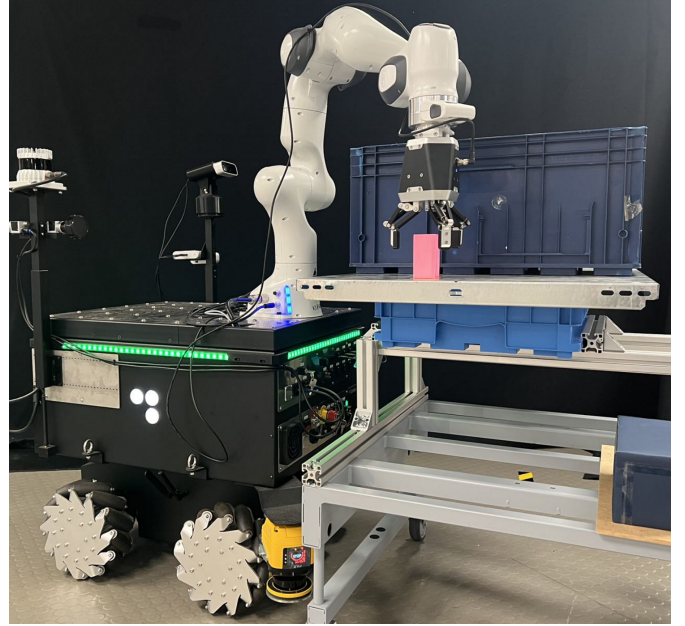


Fig. 1: FIT\* on KI-Fabrik/DARKO-Project mobile manipulator during a real-time navigation grasping task in Deutsches Museum, Munich, Germany (Section VI-B).

(RRT) [6] and Probabilistic Roadmaps (PRM) [7] construct feasible paths by randomly sampling points in the *configuration state space* (CSS) and connecting them with collision checks. These approaches are suitable for high-dimensional and complex environments.

Efficient pathfinding with high-dimensional CSS in an incremental planner hinges on balancing approximation and detachment in search. Batch Informed Trees (BIT\*) [8], [9] compactly groups states into an implicit *random geometric graph* (RGG) [10], employing step-wise search akin to Life-long Planning A\* (LPA\*) [11] based on expected solution quality. Effort Informed Trees (EIT\*) [12], a state-of-the-art planner in informed planning, uses admissible cost and effort heuristics, similar to BIT\*, Advanced BIT (ABIT\*) [13], and Adaptively Informed Trees (AIT\*) [12], [14]. However, a common limitation among these almost-surely anytime algorithms is the lack of adaptability in selecting an optimal batch size during the planning process, especially concerning the initial path finding and optimization stage. This limitation hampers overall planning efficiency [9].

This paper presents Flexible Informed Tree (FIT\*), an extension of EIT\* that integrates the strengths of both *search strategies* and *approximation techniques* within the domain of sampling-based planning. FIT\* aims to synergize these features to achieve a comprehensive and efficient planning

<sup>1</sup>L. Zhang, Z. Bing, K. Chen, L. Chen F. Wu, S. Haddadin and A. Knoll are with the Department of Informatics, Technical University of Munich, Germany. liding.zhang@tum.de

<sup>2</sup>P. Krumbholz, Z. Yuan are with the Department of Technology & Innovation, KION Group Linde Material Handling GmbH, Germany.

approach. By seamlessly integrating deep learning techniques, employing sigmoid functions for dynamic batch size adjustments, FIT\* effectively manages batch sizes and refines approximations within an increasingly dense RGG. This integration enhances the accuracy and efficiency of the approximation process.

The practical efficacy of FIT\* has been thoroughly demonstrated through rigorous real-world applications, particularly at DARKO/KI-Fabrik, as previously depicted in Figures 1. In a series of field tests and routing tasks conducted at the Deutsches Museum, we evaluate autonomous mobile manipulator navigation performance. Its adaptability in dynamically adjusting batch sizes during the optimization process demonstrated notable enhancements in computational time efficiency. FIT\* emerged as a pioneering solution, addressing the limitation seen in existing algorithms like EIT\*, BIT\*, ABIT\*, and AIT\* by enabling appropriate batch size selection during optimization. FIT\* is a promising and leading-edge solution for advancing autonomous robotic navigation, especially in dynamic, and densely populated settings. The robustness and effectiveness of FIT\* underline its potential to the field of autonomous robotics and path planning.

The contributions of this work are summarized as follows:

- *Efficient planning*: FIT\*'s adaptive batch size algorithm optimizes the computational effort of the initial solution, reducing the initial feasible pathfinding time in Random Rectangles  $\mathbb{R}^2$  up to approx. 24.2%.
- *Improved path quality*: The algorithm enhances the resolution of the approximation, resulting in shorter solution paths and more accurate solutions in pathfinding.
- *Adaptability to complex environments*: FIT\* efficiently balances accuracy and computational demands, making it highly adaptable to dynamic and high-dimensional environments.

## II. RELATED WORK

Effective motion planning involves striking a balance between exploration and exploitation. Overemphasizing exploration may waste time mapping the environment without progressing towards the goal, while an excessive focus on exploitation may overlook potentially superior solutions. It's essential to dynamically integrate exploration for information gathering and exploitation for optimal decision-making based on available knowledge in motion planning [15]. Rickert et al. strive to achieve a balance between exploration and exploitation in their Exploring/Exploiting Trees (EET) [16] algorithm by incorporating gradient information.

Multi-query algorithms, such as PRM and PRM\* [15], construct a graph roadmap in the robot's configuration space by randomly sampling configurations and connecting collision-free points. Through iterative optimization, they approximate a near-optimal path, effectively balancing exploration and exploitation for efficient and high-quality robot navigation. Lazy Probabilistic Roadmap (Lazy-PRM) [18] improves roadmap construction by deferring collision checking until necessary for a specific path. In contrast to traditional PRM, which assumes initial collision-free states and checks collisions during roadmap construction, Lazy-PRM delays this process until

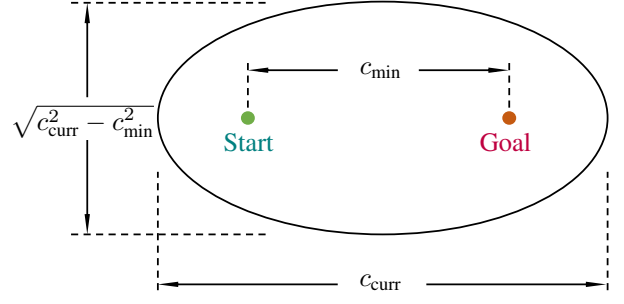


Fig. 2: The hyperellipsoid's shape is determined by the start and goal states, as well as two key costs: the theoretical minimum cost  $c_{\min}$  and the current best solution cost  $c_{\text{curr}}$ . The eccentricity of the hyperellipsoid is given by the ratio  $c_{\min}/c_{\text{curr}}$  [17].

essential for path planning. This strategic approach considerably enhances efficiency, expedites roadmap construction, and optimizes computational resources by checking collisions only as required.

Single query in path planning involves a robot finding the shortest or fastest path to reach a goal while avoiding obstacles. Rapidly-Exploring Random Trees (RRT) method incrementally expands a tree from the starting state, quickly exploring uncharted regions in the state space using random sampling and a bias towards unexplored areas. RRT-Connect extends RRT to efficiently find a path between two points in CSS by utilizing two RRTs to connect the start and goal states, progressively building a *greedy tree* for a feasible path. It iteratively extends the trees, ensuring optimality and completeness. RRT\* [15] enhances efficiency and optimality by incrementally constructing a tree from an initial state, favoring exploration towards uncharted areas. Informed-RRT\* [17] and Smart-RRT\* [19], extensions of RRT\*, employ heuristics or informed sampling (Fig. 2) to guide state space exploration, biasing sampling towards regions likely to contain the optimal path. This strategic approach speeds up path planning, especially beneficial for feasible path optimizations.

BIT\* is a sampling-based planner designed to achieve almost-surely asymptotic optimality. It constructs a discrete approximation of the CSS by sampling states in batches. This approximation is concentrated on the state space region that has the potential to enhance the current solution, using informed sampling [20] techniques.

BIT\* utilizes a *batch processing approach*, takes numerous state batches and perceives the resultant approximation as a progressively denser edge-implicit Random Geometric Graph. It optimizes the tree structure iteratively to minimize computational overhead. EIT\* and AIT\* consist of forward edge build and reverse search to employ distinct heuristic approaches for pathfinding. AIT\* excels in precision by updating its heuristic with high accuracy to match the ongoing approximation. EIT\* is built on BIT\* and uses effort as an additional heuristic function to estimate the collision check of the edges. In contrast, EIT\* focuses on optimizing the pathfinding process by utilizing the count *number of collision checks* as an effort estimate heuristic, leading to refined and efficient path discovery.

Open Motion Planning Library (OMPL) [21], is a widely used open-source software designed to address motion plan-

ning challenges in robotics and related fields. It provides a comprehensive framework and a suite of tools to assist researchers and developers in developing efficient motion planning algorithms. In our effort to improve motion planning capabilities, we integrated our innovative algorithm, Flexible Informed Tree (FIT\*), into the OMPL framework and Planner-Arena benchmark database [22], along with Planner Developer Tools (PDT) [23].

### III. PROBLEM FORMULATION

We define the problem of optimal planning in a manner associated with the definition provided in [15].

*Problem Definition 1 (Optimal Planning):* Consider a planning problem with the state space  $X \subseteq \mathbb{R}^n$ . Let  $X_{\text{obs}} \subset X$  represent states in collision with obstacles, and  $X_{\text{free}} = cl(X \setminus X_{\text{obs}})$  denote the resulting permissible states, where  $cl(\cdot)$  represents the *closure* of a set. The initial state is denoted by  $\mathbf{x}_{\text{start}} \in X_{\text{free}}$ , and the set of desired final states is  $X_{\text{goal}} \subset X_{\text{free}}$ . A sequence of states  $\sigma : [0, 1] \mapsto X$  forms a continuous map (i.e., a collision-free, feasible path), and  $\Sigma$  represents the set of all nontrivial paths.

The optimal solution, represented as  $\sigma^*$ , corresponds to the path that minimizes a selected cost function  $s : \Sigma \mapsto \mathbb{R}_{\geq 0}$ . This path connects the initial state  $\mathbf{x}_{\text{start}}$  to any goal state  $\mathbf{x}_{\text{goal}} \in X_{\text{goal}}$  through the free space:

$$\sigma^* = \arg \min_{\sigma \in \Sigma} \{s(\sigma) | \sigma(0) = \mathbf{x}_{\text{start}}, \sigma(1) \in \mathbf{x}_{\text{goal}}, \forall t \in [0, 1], \sigma(t) \in X_{\text{free}}\} \quad (1)$$

where  $\mathbb{R}_{\geq 0}$  denotes non-negative real numbers. The cost of the optimal path is  $s^*$ .

Considering a discrete set of states,  $X_{\text{samples}} \subset X$ , as a graph where edges are determined algorithmically by a transition function, we can describe its properties using a probabilistic model implicit dense RGGs when these states are randomly sampled, i.e.,  $X_{\text{samples}} = \{\mathbf{x} \sim \mathcal{U}(X)\}$ , as discussed in [10].

The characteristics of anytime almost-surely sampling-based planner with the definition are provided in [20].

*Problem Definition 2 (Almost-sure asymptotic optimality):* A planner is considered almost-surely asymptotically optimal as the number of samples tends to *infinity* which covers the entire general CSS. In this scenario, if an optimum solution exists (as definition 1 optimal planning), the probability of the planner asymptotically converging to the optimal solution nears certainty, approaching a probability of one.

$$P\left(\limsup_{q \rightarrow \infty} c(\sigma_q) = c(\sigma^*)\right) = 1 \quad (2)$$

where  $q$  represents the number of samples per batch-size,  $\sigma_q$  signifies the path derived by the planner from those batch of samples,  $\sigma^*$  stands for the optimal solution to the planning problem, and  $c(\cdot)$  denotes the path's cost at the informed batch. After discovering a initial solution, the set of states has the opportunity to utilize the remaining computational time to optimize the path quality of existing solution.

### IV. FLEXIBLE INFORMED TREES (FIT\*)

FIT\* builds on EIT\* and follows the same fundamental three-step process as EIT\* (Algorithm 1): (i) refining the

---

#### Algorithm 1: Asymmetric bidirectional search

---

```

1 repeat
2   improve RGG approximation (re-sampling)
3   update current batch size (adaptive adjust)
4   calculate heuristics (reverse search)
5   while RGG approximation is beneficial do
6     discover the feasible path (forward search)
7     if found invalid edge or unprocessed state
8       update heuristics (reverse search)
9 until planner termination condition

```

---

RGG approximation through re-sampling, (ii) computing the heuristics through reverse search, and (iii) identifying valid paths within the present RGG approximation through forward search. Just like EIT\*, FIT\* iteratively enhances the state space approximation using a sequence of denser RGGs, and if the reverse search concludes without reaching the start, it omits the forward search. However, FIT\* and EIT\* vary in their approach of sampling-based planning. FIT\* dynamically adjusts batch sizes based on the state space's geometry, fine-tuning the sampling density accordingly. Conversely, EIT\* adheres to a fixed batch size strategy, lacking the adaptability characteristic of FIT\*. This variance in sampling strategy results in distinct efficiencies and computational performance within motion planning algorithms.

#### A. Notation

The state space of the planning problem is denoted by  $X \subseteq \mathbb{R}^n$ , where  $n \in \mathbb{N}$ , the start by  $\mathbf{x}_{\text{init}} \in X$  and the goals by  $X_{\text{goal}} \subset X$ . The sampled states are denoted by  $X_{\text{sampled}}$ . The forward and reverse search trees are denoted by  $\mathcal{F} = (V_{\mathcal{F}}, E_{\mathcal{F}})$  and  $\mathcal{R} = (V_{\mathcal{R}}, E_{\mathcal{R}})$ , respectively. The vertices in these trees, denoted by  $V_{\mathcal{F}}$  and  $V_{\mathcal{R}}$ , are associated with valid states. The edges in the forward tree,  $E_{\mathcal{F}} \subset V_{\mathcal{F}} \times V_{\mathcal{F}}$ , represent valid connections between states, while the edges in the reverse tree,  $E_{\mathcal{R}} \subset V_{\mathcal{R}} \times V_{\mathcal{R}}$ , can lead through invalid regions of the problem domain. An edge consists of a source state,  $\mathbf{x}_s$ , and a target state,  $\mathbf{x}_t$ , and is denoted as  $(\mathbf{x}_s, \mathbf{x}_t)$ .  $\mathcal{Q}_{\mathcal{F}}$  and  $\mathcal{Q}_{\mathcal{R}}$  designate the edge-queue for the forward search and reverse search, respectively.

The function  $c : X \times X \rightarrow [0, \infty)$  represents the genuine cost of connection between two states, while a valid estimation of this cost is represented by the function  $\hat{c} : X \times X \rightarrow [0, \infty)$ . In other words,  $\forall \mathbf{x}_i, \mathbf{x}_j \in X, \hat{c}(\mathbf{x}_i, \mathbf{x}_j) \leq c(\mathbf{x}_i, \mathbf{x}_j)$ . The estimations of the cost to reach a particular state from the initial point, known as admissible cost heuristics, are denoted by the function  $\hat{g} : X \rightarrow [0, \infty)$  and are often defined as  $\hat{g}(\mathbf{x}) := \hat{c}(\mathbf{x}_{\text{start}}, \mathbf{x})$ . Similarly, admissible cost heuristics for reaching the goal from a specific state are denoted by the function  $\hat{h} : X \rightarrow [0, \infty)$  and are typically defined as  $\hat{h}(\mathbf{x}) := \min_{\mathbf{x}_{\text{goal}} \in X_{\text{goal}}} \{\hat{c}(\mathbf{x}, \mathbf{x}_{\text{goal}})\}$ .

In the context of traversing from the initial point to a specific state through the forward tree, the associated cost is denoted by  $g_{\mathcal{F}} : X \rightarrow [0, \infty)$ . This cost is precisely defined for states linked to a vertex in the forward tree and is considered infinite for states lacking such linkage. An admissible estimate for the journey's cost from start to goal, passing through a particular

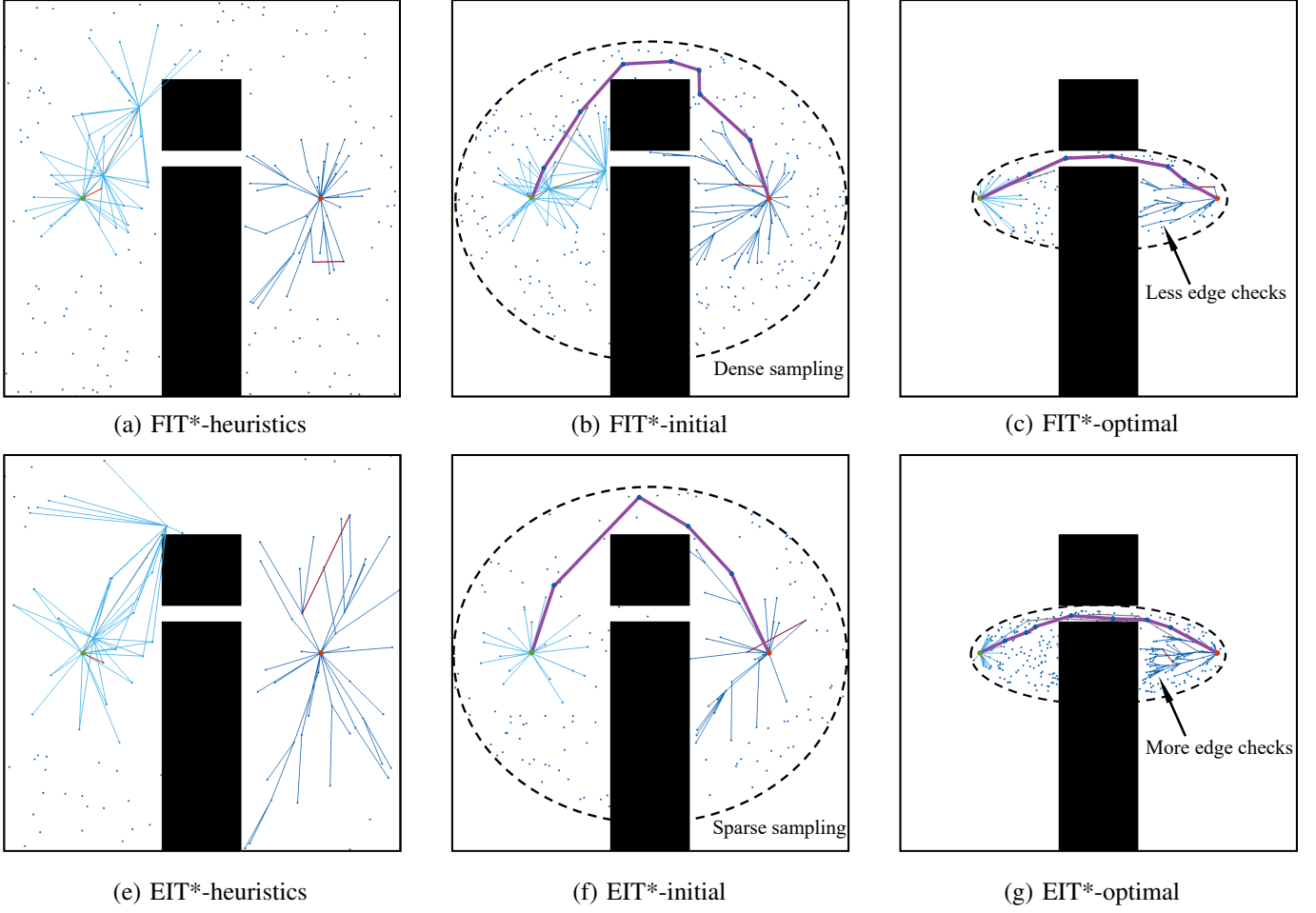


Fig. 3: Six snapshots of how FIT\* and EIT\* search a planning problem when optimizing path length. FIT\* employs an adaptive batch size strategy, focusing on larger  $n$ -dimensional hyperellipsoids to sample more points, adjusting smoothly based on edge-implicit RGG regression. The number of samples is influenced by the ellipse’s eccentricity in Figures 2. Conversely, EIT\* maintains a constant batch size across all sample batches. The approach begins with initializing the approximation and calculating cost and effort heuristics through a reverse search without full edge evaluation (a) and (e). Subsequently, both FIT\* and EIT\* pursue the resolution-optimal solution via forward search. They refine the RGG approximation through sampling and pruning, updating the heuristic accordingly (b) and (f). Finally, they utilize this refined heuristic in subsequent forward searches, correcting for invalid edges when encountered (c) and (g).

state, is approximated using  $\hat{f} : X \rightarrow [0, \infty)$ . Typically, this estimation is computed as  $\hat{f}(\mathbf{x}) := \hat{g}(\mathbf{x}) + \hat{h}(\mathbf{x})$ . This estimate defines the informed set, denoted as  $X_{\hat{f}} := \{\mathbf{x} \in X | \hat{f}(\mathbf{x}) < c_{\text{current}}\}$ , where  $c_{\text{current}}$  is the cost of the current solution,  $c_{\text{last}}$  is the cost of the last valid solution. The informed set encompasses states that have the potential to enhance the current solution.

Efficiencies in effort estimation between states are indicated by the function  $\bar{e} : X \times X \rightarrow [0, \infty)$ , providing insight into the computational effort needed to identify and validate a path, often indicating the number of collision detections required along the path. Additionally, potential inaccuracies in effort estimation between individual states and the starting state are denoted by  $\bar{d} : X \rightarrow [0, \infty)$ , usually defined as  $\bar{d}(x) := \bar{e}(\mathbf{x}, \mathbf{x}_{\text{start}})$ . Concerning cost estimation, potential inaccuracies between two states are denoted by  $\bar{c} : X \times X \rightarrow [0, \infty)$ . We assume that this estimation is never less than its admissible counterpart, i.e.,  $\forall \mathbf{x}_1, \mathbf{x}_2 \in X, \hat{c}(\mathbf{x}_1, \mathbf{x}_2) \leq \bar{c}(\mathbf{x}_1, \mathbf{x}_2)$ .

Let  $A$  be a set and let  $B, C$  be subsets of  $A$ . The notation  $B \stackrel{+}{\leftarrow} C$  is used to denote  $B \leftarrow B \cup C$  and  $B \stackrel{-}{\leftarrow} C$  is used to

denote  $B \leftarrow B \setminus C$ .

*FIT\*-specific Notation:* To incorporate decay into the process, we introduce a decay factor represented by  $\Psi_{\text{decay}}$ , alongside specifying the minimal  $m_{\min} := 1$  and maximal  $m_{\max}$  sample numbers per batch. The initial set of batch sizes, denoted as  $\mathcal{M}_{\text{init}}$ , and the current count of states sampled per batch, denoted as  $\mathcal{M}(\Psi_{\text{current}})$ . We utilize  $\zeta_n$  to symbolize the Lebesgue measure within an  $n$ -dimensional hyperellipsoid.  $\xi_n$  represents the raw ratio of the initial hypervolume of the  $n$ -dimensional hyperellipsoid  $\mathcal{V}_{\text{init}}$  to the current hypervolume  $\mathcal{V}_{\text{curr}}$ . Additionally, we introduce a logarithmic decay factor, denoted as  $\Lambda$ , which helps regulate the rate at which the ratio decreases. Furthermore, we define  $\mathcal{O}_{\text{smooth}}$  to represent a smoothed value after the sigmoid function is applied to the initial state.

### B. Initialization

FIT\* starts with an initial state as the root, constructing a search tree using an edge-queue variant of Anytime Explicit Estimation Search (AEES) [24]. AEES utilizes cost and effort heuristics from FIT\*’s reverse search in an anytime manner,



---

**Algorithm 2: EIT\* with changes for FIT\***


---

```

1   $c_{current} \leftarrow \infty; \Psi_{decay} \leftarrow \infty; \Lambda_{const.}$ 
2   $\mathcal{M}_{init} \leftarrow \mathcal{M}(\Psi_{current}); \mathcal{V}_{curr} \leftarrow \mathcal{V}_{init}; \xi_{init} := 1$   $\triangleright$  initial batch size
3   $X_{sampled} \leftarrow X_{goal} \cup \{x_{start}\}$ 
4   $V_{\mathcal{F}} \leftarrow x_{start}; E_{\mathcal{F}} \leftarrow \emptyset; Q_{\mathcal{F}} \leftarrow \emptyset$ 
5   $V_{\mathcal{R}} \leftarrow X_{goal}; V_{\mathcal{R},closed} \leftarrow \emptyset; E_{\mathcal{R}} \leftarrow \emptyset; Q_{\mathcal{R}} \leftarrow \emptyset$ 
6   $Q_{\mathcal{F}} \leftarrow \text{expand}(x_{start}); Q_{\mathcal{R}} \leftarrow \text{expand}(X_{goal})$ 
7   $\varepsilon_i \leftarrow \text{updateInfaltionFactor}()$ 
8   $d \leftarrow \text{updateSparseResolution}()$ 
9  repeat
10    $\xi_n \leftarrow \text{updateRawRatio}(\mathcal{V}_{curr}, \mathcal{V}_{init})$ 
11    $\mathcal{O}_{smooth} \leftarrow \text{sigmoidFunction}(\xi_n)$   $\triangleright$  update smoothed raw ratio
12    $\Psi_{decay} \leftarrow \text{updateDecayFactor}(\mathcal{O}_{smooth}, \Lambda_{const.})$ 
13   if  $\min_{(x_s, x_t) \in Q_{\mathcal{R}}} \{\text{key}_{\mathcal{R}}^{\text{FIT}*}(x_s, x_t)\} < \min_{(x_s, x_t) \in Q_{\mathcal{F}}} \{\text{key}_{\mathcal{F}}^{\text{FIT}*}(x_s, x_t)\}$ 
14     or target of optimal edge in forward queue
15      $(x_s, x_t) \leftarrow \arg \min_{(x_s, x_t) \in Q_{\mathcal{R}}} \{\text{key}_{\mathcal{R}}^{\text{FIT}*}(x_s, x_t)\}$ 
16      $Q_{\mathcal{R}} \leftarrow (x_s, x_t)$ 
17      $V_{\mathcal{R},closed} \leftarrow x_s$ 
18     if  $\text{noCollisionsDetected}((x_s, x_t), d)$ 
19        $\bar{h}[x_t] \leftarrow \min\{\bar{h}[x_t], \bar{h}[x_s] + \bar{c}(x_s, x_t)\}$ 
20        $\bar{e}[x_t] \leftarrow \min\{\bar{h}[x_t], \bar{e}[x_s] + \bar{e}(x_s, x_t)\}$ 
21       if  $\bar{h}[x_t] > \bar{h}[x_s] + \bar{c}(x_s, x_t)$ 
22          $\bar{h}[x_t] \leftarrow \bar{h}[x_s] + \bar{c}(x_s, x_t)$ 
23         if  $x_t \in V_{\mathcal{R}}$ 
24            $E_{\mathcal{R}} \leftarrow (\text{parent}_{\mathcal{R}}(x_t), x_t)$ 
25         else
26            $V_{\mathcal{R}} \leftarrow x_t$ 
27          $E_{\mathcal{R}} \leftarrow (x_s, x_t)$ 
28          $Q_{\mathcal{R}} \leftarrow \text{expand}(x_t)$ 
29     else
30        $E_{invalid} \leftarrow \{(x_s, x_t), (x_t, x_s)\}$ 
31        $\mathcal{M}(\Psi_{current}) \leftarrow \text{adaptiveBatchSize}(\Psi_{decay}, m_{min}, m_{max})$ 
32   else if  $\min_{(x_s, x_t) \in Q_{\mathcal{F}}} \{g_{\mathcal{F}}(x_s) + \bar{c}(x_s, x_t) + \hat{h}_{con}[x_t]\} < c_{current}$ 
33      $(x_s, x_t) \leftarrow \text{getBestForwardEdge}(Q_{\mathcal{F}})$ 
34      $Q_{\mathcal{F}} \leftarrow (x_s, x_t)$ 
35     if  $(x_s, x_t) \in E_{\mathcal{F}}$ 
36        $Q_{\mathcal{F}} \leftarrow \text{expand}(x_t)$ 
37     else if  $g_{\mathcal{F}}(x_s) + \bar{c}(x_s, x_t) < g_{\mathcal{F}}(x_t)$ 
38       if  $\text{collisionFree}(x_s, x_t)$ 
39          $\xi_n \leftarrow \text{updateRawRatio}(\mathcal{V}_{curr}, \mathcal{V}_{init})$ 
40          $\mathcal{O}_{smooth} \leftarrow \text{sigmoidFunction}(\xi_n)$ 
41         if  $g_{\mathcal{F}}(x_s) + \bar{c}(x_s, x_t) + \hat{h}_{con}[x_t] < c_{current}$ 
42           if  $g_{\mathcal{F}}(x_s) + c(x_s, x_t) < g_{\mathcal{F}}(x_t)$ 
43             if  $x_t \notin V_{\mathcal{F}}$ 
44                $V_{\mathcal{F}} \leftarrow x_t$ 
45             else
46                $E_{\mathcal{F}} \leftarrow (\text{parent}_{\mathcal{F}}(x_t), x_t)$ 
47              $E_{\mathcal{F}} \leftarrow (x_s, x_t)$ 
48              $Q_{\mathcal{F}} \leftarrow \text{expand}(x_t)$ 
49           if  $\min_{x_{goal} \in X_{goal}} \{g_{\mathcal{F}}(x_{goal})\} < c_{current}$ 
50              $c_{current} \leftarrow \min_{x_{goal} \in X_{goal}} \{g_{\mathcal{F}}(x_{goal})\}$ 
51              $\varepsilon_i \leftarrow \text{updateInfaltionFactor}()$ 
52         else
53            $E_{invalid} \leftarrow \{(x_s, x_t), (x_t, x_s)\}$ 
54           if  $(x_s, x_t) \in E_{\mathcal{R}}$ 
55              $d \leftarrow \text{updateSparseResolution}()$ 
56              $V_{\mathcal{R}} \leftarrow X_{goal}; E_{\mathcal{R}} \leftarrow \emptyset$ 
57              $Q_{\mathcal{R}} \leftarrow \text{expand}(X_{goal})$ 
58   else
59      $\text{prune}(X_{sampled})$ 
60      $\mathcal{M}(\Psi_{current}) \leftarrow \text{adaptiveBatchSize}(\Psi_{decay}, m_{min}, m_{max})$ 
61      $X_{sampled} \leftarrow \text{sample}(\mathcal{M}(\Psi_{current}), c_{current})$ 
62      $V_{\mathcal{R}} \leftarrow X_{goal}; V_{\mathcal{R},closed} \leftarrow \emptyset; E_{\mathcal{R}} \leftarrow \emptyset$ 
63      $Q_{\mathcal{F}} \leftarrow \text{expand}(X_{start}); Q_{\mathcal{R}} \leftarrow \text{expand}(X_{goal})$ 
64      $d \leftarrow \text{updateSparseResolution}()$ 
65 until planner termination condition

```

---



---

**Algorithm 3: Adaptive Batch Size**


---

```

1   $m_{min} := 1, m_{max} := 2m_{current} - m_{min}$ 
2  if  $c_{current} \neq c_{last}$ 
3     $c_{last} \leftarrow c_{current}$ 
4    if pragma once
5       $\mathcal{V}_{init} \leftarrow \text{ellipseVolumCal}(c_{last})$   $\triangleright \mathcal{V}_{init}$  only calculated once
6     $\mathcal{V}_{curr} \leftarrow \text{ellipseVolumCal}(c_{current})$   $\triangleright \mathcal{V}_{curr}$  update every-time
7     $\xi_n \leftarrow \text{updateRawRatio}(\mathcal{V}_{curr}, \mathcal{V}_{init})$ 
8     $\mathcal{O}_{smooth} \leftarrow \text{sigmoidFunction}(\xi_n)$ 
9     $\Psi_{decay} \leftarrow \text{updateDecayFactor}(\mathcal{O}_{smooth}, \Lambda_{const.})$ 
10    $\mathcal{M}(\Psi_{current}) := m_{min} + \Psi_{decay}(m_{max} - m_{min})$   $\triangleright$  adapted batch size
11   return  $\mathcal{M}(\Psi_{current})$ 

```

---

established admissible cost heuristics. AEES gradually tightens suboptimality bounds through multiple searches on the same RGG approximation. Initially prioritizing speed over resolution-optimal outcomes, AEES proves beneficial when informative admissible cost heuristics are lacking, using an effort heuristic to guide the search. FIT\* refines the tree using both admissible and inadmissible cost heuristics until achieving the resolution optimum.

Upon initialization (Algorithm 2, Lines 1-8), the initial cost is set to infinity, and the default batch size is denoted as  $\mathcal{M}_{init}$ . Initially, both the raw initial ratio  $\xi_{init}$  and the ratio of current hypervolume to initial hypervolume  $\mathcal{V}_{curr}/\mathcal{V}_{init}$  are equal to one, reflecting the equivalence of the current and initial hypervolumes in the initial state.

### C. Adaptive Batch-Size

FIT\* dynamically adjusts the number of samples in batch size, taking inspiration from techniques often utilized in deep learning. Specifically, it leverages the sigmoid function in conjunction with logarithmic transformations, resembling practices commonly seen in the field.

Within the FIT\* flexible batch size context (Algorithm 3), our experimentation focused on exploring various decay methods to understand their unique impacts on the behavior of the log function and, consequently, their influence on the adaptation process. These decay methods encompassed linear decay, brachistochrone curve-based decay, decay functions following an exponential pattern, and decay based on the iteration count. Each method was thoroughly examined to assess its effectiveness in shaping the decay factor  $\Psi_{decay}$ .

Linear decay, characterized by a consistent and gradual reduction in the decay factor, offered a predictable and steady adjustment. Conversely, the brachistochrone curve, known for providing the shortest descent time between two points in a gravitational field, showcased a faster initial adjustment that gradually slowed as the process advanced. Exponential decay, a prevalent pattern in numerous natural processes, displayed an even quicker initial adjustment that gradually tapered off over time. Lastly, decay based on the iteration count demonstrated a clear correlation between the number of iterations and the rate of adjustment.

Through this extensive experimentation, it became clear that the present combination of factors and methodologies, particularly the log function combined with a sigmoid smoothing, emerged as the most efficient and effective approach.

allowing rapid initial solution generation, even without pre-

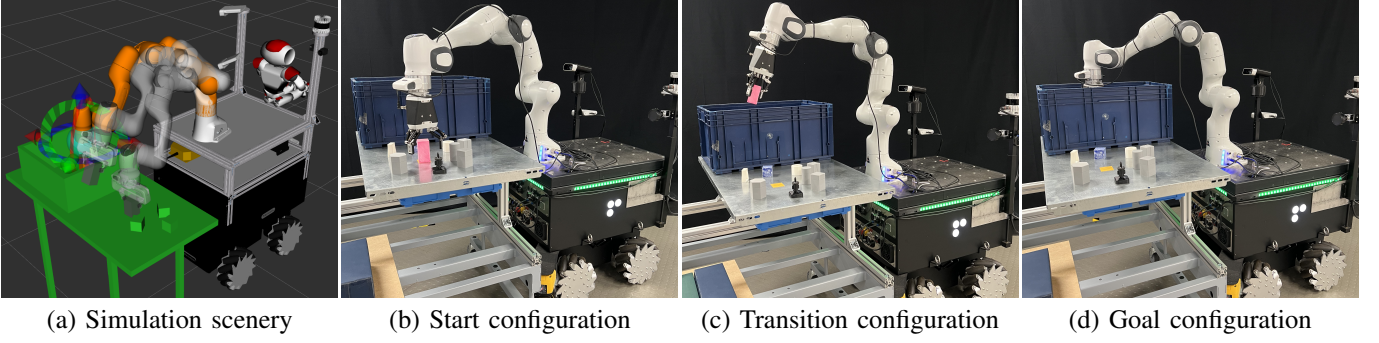


Fig. 4: Illustrates the simulation (a) and the real-world scenarios of DARKO robot for the intralogistics task, (b) shows the start configuration of the arm in position to pick up the red cube from the metal sheet table, (c) shows the transition configuration position of the task, (d) shows the goal configuration of the arm in position to place a cube in the box.

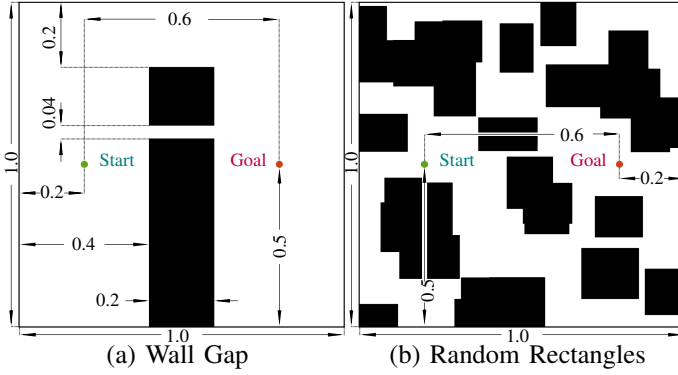


Fig. 5: In Section VI, we employed a 2D representation to illustrate the simulated planning problems. The state space, denoted as  $X \subset \mathbb{R}^n$ , is constrained within a hypercube with a width of two for both problem instances. Specifically, we conducted ten distinct instantiations of the random rectangles experiment and the outcomes are showcased in Figures 6.

This specific combination outperformed the above mentioned methods and proved optimal in determining how the decay factor  $\Psi_{\text{decay}}$  affects the log function. The logarithmic function, complemented by the smoothing effect of the sigmoid function, enabled us to achieve a delicate balance between adaptability to the denser sampling in initial phase and sparse sampling in the optimalization phase of CSS.

## V. FORMAL ANALYSIS

In this paper, we refer to Definition 24 from [15] to establish the concept of almost-sure asymptotic optimality. Addressing duplicate connection failure samples requires utilizing non-uniform distribution theories within the framework of RGG. However, our present priority is the adaptive adjustment of batch sizes, guided by RGG insights. By utilizing RGGs information to modulate batch sizes and strategically employing multiple points, we aim to enhance the efficiency of the initial solution process.

The sampling-based planner FIT\* is designed to adapt the batch size as needed, increasing the number of samples during the initial solution finding stage and accelerates the convergence of a feasible path. Conversely, reducing the number of samples per batch speeds up the optimization process by minimizing edge checks, ultimately accelerating the batch sample rate and reducing computational time. The adjustment of batch size cleverly responds to the current ratio  $\xi_n$ , aligning with

the specific problem characteristics. This alignment with the hypervolume of an  $n$ -dimensional hyperellipsoids, a critical aspect for comprehending the rationale is outlined below:

$$\xi_n = \frac{V_{\text{curr}}}{V_{\text{init}}} \quad (3)$$

Decay parameter  $\Lambda$  is computed based on the problem's dimensionality  $n_{\text{dimension}}$  along with the minimum and maximum batch sizes  $m_{\text{min}}$  and  $m_{\text{max}}$ . This factor is a composite representation, considering the semi-axial lengths, which demonstrates how the hyperellipsoids's shape plays a role in the adaptation process.

$$\Lambda = \frac{\mathcal{M}(\Psi_{\text{max}}) + \mathcal{M}(\Psi_{\text{min}})}{n_{\text{dimension}}} \quad (4)$$

The sigmoid smoothing technology of the raw ratio  $\mathcal{O}_{\text{smooth}}$  ensures a gradual transition between batch sizes, mirroring how the hyperellipsoids's hypervolume changes smoothly with varying semi-axes lengths. This smoothing function allows for a more continuous adjustment of the batch size.

$$\mathcal{O}_{\text{smooth}} = \frac{1}{1 + e^{-10 \times (\xi_n - 0.5)}} \quad (5)$$

where  $e$  is Euler's number  $e = \sum_{i=0}^{\infty} \frac{1}{i!}$

We experimented with several decay methods, including linear, brachistochrone curve, exponential function, and based on the iteration count. Through this experimentation, we found that the current combination remains the most effective in determining the influence of the decay factor  $\Psi_{\text{decay}}$  on the log function. This relationship emphasizes how the dimensions of the hyperellipsoids shape influence the exploration of the state space in a logarithmic manner.

$$\Psi_{\text{decay}} = \frac{\ln(1 + \Lambda \times \mathcal{O}_{\text{smooth}})}{\ln(1 + \Lambda)} \quad (6)$$

The adapted batch size function  $\mathcal{M}(\Psi)$  is the major influence, considering the integration of the decay factor. It reflects how stretching or compressing the hyperellipsoids in different dimensions affects the appropriate batch size, aligning with the exploration requirements.

$$\mathcal{M}(\Psi) := m_{\text{min}} + (m_{\text{max}} - m_{\text{min}}) \times \Psi_{\text{decay}} \quad (7)$$

In summery, FIT\* is an anytime adaptive sample-based planner, dynamically adjusting batch sizes for adaptability to the

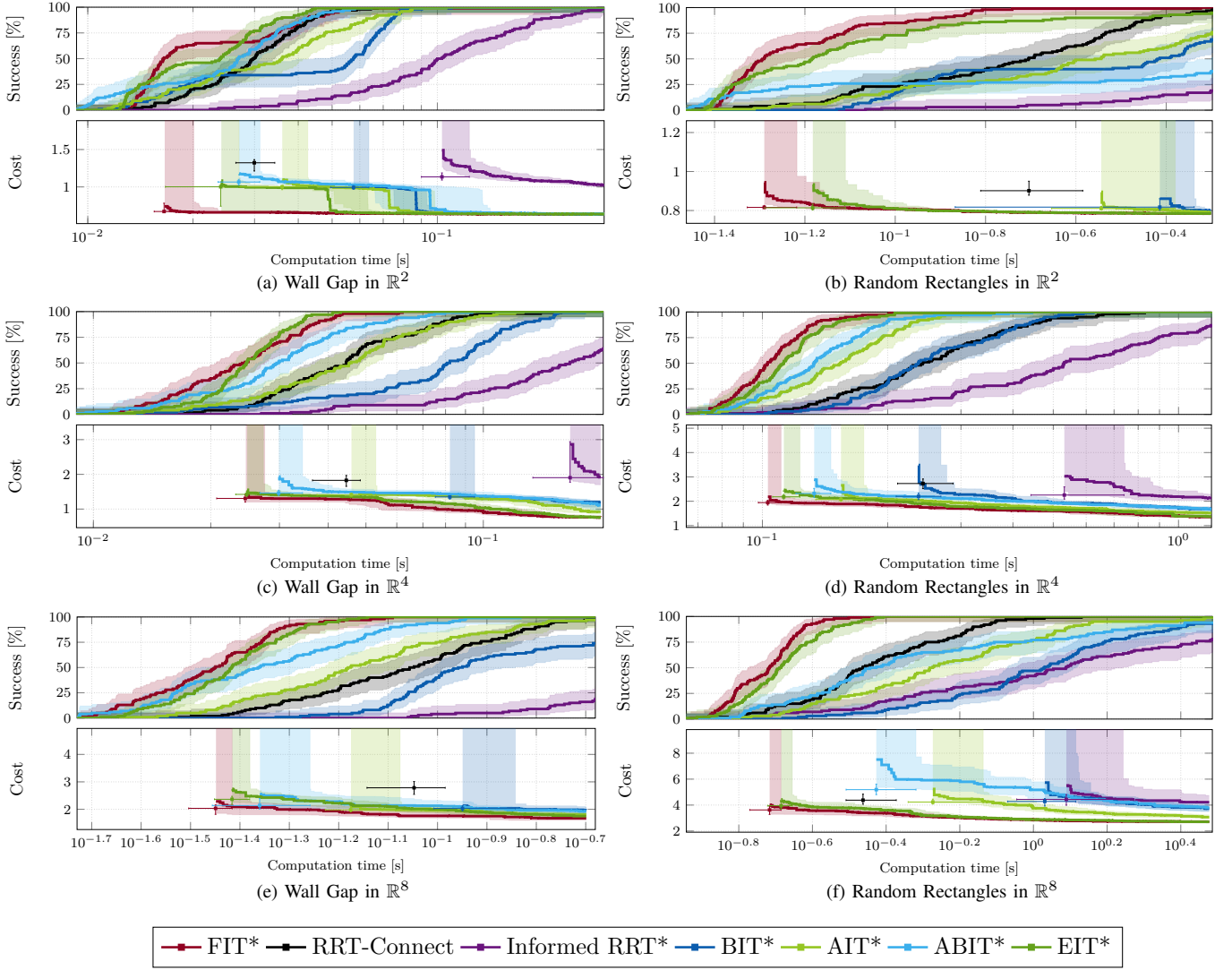


Fig. 6: Detailed experimental results from Section VI-A are presented above. Figures (a), (c) and (e) depict test benchmark wall gap outcomes in  $\mathbb{R}^2$ ,  $\mathbb{R}^4$  and  $\mathbb{R}^8$ , respectively. Panel (b) showcases ten random rectangle experiments in  $\mathbb{R}^2$ , while panels (d) and (f) demonstrate in  $\mathbb{R}^4$  and  $\mathbb{R}^8$ . In the cost plots, boxes represent solution cost and time, with lines showing cost progression for an almost surely asymptotically optimal planner (unsuccessful runs have infinite cost). Error bars provide nonparametric 99% confidence intervals for solution cost and time.

CSS. It effectively addresses complex scenarios and utilizes  $n$ -dimensional hyperellipsoid properties to enhance efficiency and optimality in motion planning.

## VI. EXPERIMENTAL RESULTS

FIT\* was compared against versions of RRT-Connect, Informed RRT\*, BIT\*, AIT\*, ABIT\*, and EIT\* from the Open Motion Planning Library (OMPL) [21]. These comparisons were carried out in simulated environments ranging from  $\mathbb{R}^2$  to  $\mathbb{R}^8$ . The primary objective for the planners with almost-surely asymptotic optimality was to minimize path length. The RGG constant  $\eta$  was uniformly set to 1.1, and the rewiring factor was consistently set to 1.001 for all planners.

In the case of RRT-based algorithms, a goal bias of 5% was employed, and the maximum edge lengths were appropriately determined based on the dimensionality of the space. Conversely, BIT\*, AIT\*, ABIT\*, and EIT\* maintained a fixed sampling of 100 states per batch, irrespective of the dimensionality of the state space. These planners also had graph pruning deactivated and utilized the Euclidean distance as a

heuristic. FIT\*'s adaptive batch size technology dynamically adjusts the batch size, displaying a range from 1 to 199 batch sizes. The specific number of samples at anytime is determined by the planner's adaptive mechanisms, ensuring quantities that are optimized for each batch.

### A. Experimental Tasks

The planners were subjected to testing across three distinct problem domains:  $\mathbb{R}^2$ ,  $\mathbb{R}^4$ , and  $\mathbb{R}^8$ . In the first scenario, a constrained environment resembling a wall with a narrow gap was simulated, allowing valid paths in only two distinct homotopy classes (Fig. 5a). Each planner underwent 100 runs, each lasting under one second, with varying random seeds. The success rates and median path lengths for all planners are depicted in Figures 6a, 6c, and 6e.

In the second test environment, random widths were assigned to *axis-aligned hyperrectangles*, which were generated within the CSS arbitrarily (Fig. 5b). Unique random problems were created for each dimension of the CSS, and each planner was run 100 times for every instance. Figures 6b, 6d, and

6f present the success rates and median path costs of all the planners.

### B. Planning for DARKO-robot

FIT\* demonstrated its effective adaptive batch size techniques during a field test in the Deutsches Museum Munich as part of the DARKO project (Fig. 1 and Fig. 4). DARKO, a mobile manipulation robotic platform created by combining Robotnik RB-KAIROS+ base robot and Franka Emika Panda manipulator, addresses intralogistics supermarket challenges. The complex terrain, creates challenging planning problems due to computationally expensive state evaluations. FIT\* consistently obtained initial solutions for these intricate problems within seconds to further optimize its approach, improving initial solution time and reducing path length with the remaining computational time. Detailed behavior of DARKO can be viewed in the accompanying video.

## VII. DISCUSSION & CONCLUSION

FIT\* introduces a groundbreaking feature - adaptive batch size, revolutionizing path planning. dynamically adjusting batch sizes based on the inherent complexity of the planning domain and the current  $n$ -dimensional hyperellipsoid of the system. In comparative assessments, FIT\* outperforms planners with fixed batch sizes by displaying constantly update optimized batch sizes. During the heuristic discovery phase illustrated in (Fig. 3), increasing the number of samples per batch led to faster discovery of the initial solution. Conversely, during the optimal phase, providing fewer samples per batch reduced collision checking calculation time, thereby enhancing the sampling efficiency for multiple batches. FIT\* consistently achieved higher success rates and shorter both initial and optimal path lengths in various testing scenario settings, demonstrating its efficiency in both constrained and randomly structured complex environments.

The adaptability of FIT\* was exemplified in a real-world scenario, planning for the DARKO-Robot. FIT\*'s adaptive strategies ensured rapid initial solutions. This adaptability empowered autonomous navigation through challenging terrains, illustrating FIT\*'s practical applicability and practical industry problem-solving capacity.

In conclusion, FIT\* employs a flexible approach by dynamically adjusting batch sizes based on the inherent complexity of the planning domain and the current  $n$ -dimensional hyperellipsoid of the system. The potential to appropriately adjust batch sizes demonstrates the ability to optimize the algorithmic process by modifying number of sampling points per batch and batch updating frequency. This feature positions FIT\* as a promising solution in the field of path planning.

## REFERENCES

- [1] E. Dijkstra, "A note on two problems in connexion with graphs," *Numerische Mathematik*, vol. 1, no. 1, pp. 269–271, 1959.
- [2] P. E. Hart, N. J. Nilsson, and B. Raphael, "A formal basis for the heuristic determination of minimum cost paths," *IEEE transactions on Systems Science and Cybernetics*, vol. 4, no. 2, pp. 100–107, 1968.
- [3] M. Likhachev, G. J. Gordon, and S. Thrun, "Ara\*: Anytime a\* with provable bounds on sub-optimality," *Advances in neural information processing systems*, vol. 16, 2003.
- [4] D. Bertsekas, "Convergence of discretization procedures in dynamic programming," *IEEE Transactions on Automatic Control*, vol. 20, no. 3, pp. 415–419, 1975.
- [5] R. Bellman, "Dynamic programming, princeton univ," *Press Princeton, New Jersey*, 1957.
- [6] S. M. LaValle and J. J. Kuffner Jr, "Randomized kinodynamic planning," *The international journal of robotics research*, vol. 20, no. 5, pp. 378–400, 2001.
- [7] L. E. Kavraki, P. Svestka, J.-C. Latombe, and M. H. Overmars, "Probabilistic roadmaps for path planning in high-dimensional configuration spaces," *IEEE transactions on Robotics and Automation*, vol. 12, no. 4, pp. 566–580, 1996.
- [8] J. D. Gammell, S. S. Srinivasa, and T. D. Barfoot, "Batch informed trees (bit\*): Sampling-based optimal planning via the heuristically guided search of implicit random geometric graphs," in *2015 IEEE international conference on robotics and automation (ICRA)*. IEEE, 2015, pp. 3067–3074.
- [9] J. D. Gammell, T. D. Barfoot, and S. S. Srinivasa, "Batch informed trees (bit\*): Informed asymptotically optimal anytime search," *The International Journal of Robotics Research*, vol. 39, no. 5, pp. 543–567, 2020.
- [10] M. Penrose, *Random geometric graphs*. OUP Oxford, 2003, vol. 5.
- [11] S. Koenig, M. Likhachev, and D. Furcy, "Lifelong planning a\*," *Artificial Intelligence*, vol. 155, no. 1-2, pp. 93–146, 2004.
- [12] M. P. Strub and J. D. Gammell, "Adaptively informed trees (ait\*) and effort informed trees (eit\*): Asymmetric bidirectional sampling-based path planning," *The International Journal of Robotics Research*, vol. 41, no. 4, pp. 390–417, 2022.
- [13] M. P. Strub and J. D. Gammell, "Advanced bit (abit): Sampling-based planning with advanced graph-search techniques," in *2020 IEEE International Conference on Robotics and Automation (ICRA)*. IEEE, 2020, pp. 130–136.
- [14] M. P. Strub and J. D. Gammell, "Adaptively informed trees (ait): Fast asymptotically optimal path planning through adaptive heuristics," in *2020 IEEE International Conference on Robotics and Automation (ICRA)*. IEEE, 2020, pp. 3191–3198.
- [15] S. Karaman and E. Frazzoli, "Sampling-based algorithms for optimal motion planning," *The international journal of robotics research*, vol. 30, no. 7, pp. 846–894, 2011.
- [16] M. Rickert, O. Brock, and A. Knoll, "Balancing exploration and exploitation in motion planning," in *2008 IEEE International Conference on Robotics and Automation*. IEEE, 2008, pp. 2812–2817.
- [17] J. D. Gammell, S. S. Srinivasa, and T. D. Barfoot, "Informed rrt: Optimal sampling-based path planning focused via direct sampling of an admissible ellipsoidal heuristic," in *2014 IEEE/RSJ international conference on intelligent robots and systems*. IEEE, 2014, pp. 2997–3004.
- [18] R. Bohlin and L. E. Kavraki, "Path planning using lazy prm," in *Proceedings 2000 ICRA. Millennium conference. IEEE international conference on robotics and automation. Symposia proceedings (Cat. No. 00CH37065)*, vol. 1. IEEE, 2000, pp. 521–528.
- [19] J. Nasir, F. Islam, U. Malik, Y. Ayaz, O. Hasan, M. Khan, and M. S. Muhammad, "Rrt\*-smart: A rapid convergence implementation of rrt," *International Journal of Advanced Robotic Systems*, vol. 10, no. 7, p. 299, 2013.
- [20] J. D. Gammell, T. D. Barfoot, and S. S. Srinivasa, "Informed sampling for asymptotically optimal path planning," *IEEE Transactions on Robotics*, vol. 34, no. 4, pp. 966–984, 2018.
- [21] I. A. Sucan, M. Moll, and L. E. Kavraki, "The open motion planning library," *IEEE Robotics & Automation Magazine*, vol. 19, no. 4, pp. 72–82, 2012.
- [22] M. Moll, I. A. Sucan, and L. E. Kavraki, "Benchmarking motion planning algorithms: An extensible infrastructure for analysis and visualization," *IEEE Robotics & Automation Magazine*, vol. 22, no. 3, pp. 96–102, 2015.
- [23] J. D. Gammell, M. P. Strub, and V. N. Hartmann, "Planner developer tools (pdt): Reproducible experiments and statistical analysis for developing and testing motion planners," in *Proceedings of the Workshop on Evaluating Motion Planning Performance (EMPP), IEEE/RSJ International Conference on Intelligent Robots and Systems (IROS)*, 2022.
- [24] J. Thayer, J. Benton, and M. Helmert, "Better parameter-free anytime search by minimizing time between solutions," in *Proceedings of the International Symposium on Combinatorial Search*, vol. 3, no. 1, 2012, pp. 120–128.